DEVELOPMENT OF PRE-CLINICAL MURINE MODELS FOR FIBROLAMELLAR HEPATOCELLULAR CARCINOMA

Andy He[1,2*], Garry L. Coles[1,2*], Griffin G. Hartmann[1,2], Julia Arand[1,2,3], Vicky Le[1,2], Brandon Mauch[1,2], Lei Xu[1,2], Thuyen Nguyen[1,2], Florette K. Hazard[1,4], and Julien Sage[1,2#]

Departments of [1]Pediatrics, [2]Genetics, and [4]Pathology, Stanford University School of Medicine, Stanford, CA, USA. [3]Department of Cell and Developmental Biology, Center of Anatomy and Cell Biology, Medical University of Vienna, 1090, Vienna, Austria.

* Equal contribution

#Correspondence: julsage@stanford.edu

Authors Contributions: G.L.C. and J.S. designed the project together, with initial input from L.X.; G.L.C. performed most of the experiments related to characterizing the transgenic mice, with help from V.L., B.M., T.N., and A.H.; A.H. performed most of the experiments related to *ex vivo* culture assays; F.K.H. performed histopathological analyses; J.A. and G.G.H. analyzed the RNA sequencing data for embryonic livers and tumors, respectively; G.L.C., A.H., G.G.H., and J.S. interpreted the experiments together; A.H., and J.S. wrote the manuscript and prepared the figures with contributions from all authors.

Keywords: fibrolamellar carcinoma, liver, cancer, PKA, organoids, mouse models

ABSTRACT

Fibrolamellar hepatocellular carcinoma (FLC) is a rare form of cancer that affects primarily adolescents and young adults. FLC tumors are typically associated with an intrachromosomal deletion resulting in expression of a fusion protein between the chaperone DNAJ1B and the protein kinase PKA. FLC is challenging to study because of its rarity and limited pre-clinical models. Here we developed a novel transgenic mouse model of FLC. In this model, DNAJ1B-PKA expression in the liver of mouse embryos results in perinatal lethality associated with liver developmental defects, while DNAJ1B-PKA expression in the liver of adult mice initiates tumors resembling FLC at low penetrance. We sought to develop *ex vivo* cell models from these tumors but failed to establish long-term cell lines. New pre-clinical models of FLC will provide novel insights into the biology of this rare cancer and may help identify novel therapeutic strategies.

INTRODUCTION

While hepatocellular carcinoma (HCC) in adults is a leading cause of mortality worldwide [1], liver cancer is much rarer in children and young adults. A majority of pediatric liver cancer cases are hepatoblastomas but primary HCCs are sometimes diagnosed [2]. In particular, fibrolamellar hepatocellular carcinoma (FL-HCC, or FLC) is a very rare and distinct subtype of HCC that affects adolescents and young adults. FLC develops in the setting of normal healthy livers, with no known genetic predisposition factor [3-5]. FLC is associated with better survival than HCC in adults, presumably due to the young age of the patients and the lack of cirrhosis, which makes more aggressive surgery possible [6]. However, few therapeutic options have been successfully explored beyond surgery. The 5-year survival rate ranges from 35-75% in patients treated with liver transplantation or resection. In cases where surgery is not possible, the survival drops to 12-14 months [7-10].

Morphologically, FLC tumors are characterized by pleomorphic malignant hepatocytes with large central nucleoli and abundant eosinophilic cytoplasm. The cancer cells are arranged in variably sized nests or cords set within a meshwork of lamellated collagen fibers. In the majority of cases, FLC cells contain hyaline droplets and some isolated cells have round cytoplasmic inclusions known as “pale bodies” [11, 12]. FLC express markers associated with biliary (e.g., CK7 and MUC1) and hepatocytic (e.g., Heppar-1, Albumin, α-1-antitrypsin, and Glypican-3) differentiation, as well as hepatic progenitor/stem cells (e.g., CK19, EPCAM) [3, 13-19].

At the genetic level, a breakthrough in the field was the discovery of a fusion event resulting in high levels of the catalytic subunit of PKA (protein kinase A) in FLC tumors [20, 21]. This finding was confirmed in other studies [22-24]. Rare cases of FLC have been associated with genetic inactivation of *PRKAR1A*, which encodes a regulatory subunit of PKA [25]. Rare cases of *BAP1* mutant HCC also have features of FLC and show amplification of the *PRKACA* gene coding for PKA with no fusion event [26]. Thus, high PKA activity may be sufficient to drive FLC development. Indeed, expression of PKA in the liver of young adult mice is sufficient to initiate tumors resembling FLC [27, 28]. In addition, inhibition of PKA kinase activity has anti-tumor activity against pre-

clinical models of FLC [29] and knock-down of the fusion protein inhibits the growth of patient-derived xenografts [30]. However, the small part of DNAJ1B fused to PKA in FLC tumors also contributes to tumor development in mice [27], an observation supported by biochemical and structural studies [31-36]. Few additional alterations have been found in the genome of FLC tumors, but accumulating evidence suggests a role for telomerase activity, MAPK signaling, and WNT signaling [26, 27, 35, 37-41].

The very low incidence rate of 0.02 per 100,000 has kept FLC an understudied cancer [42]. Very few cell lines and patient-derived xenograft models remain available, and these models often do not propagate easily, even though they can provide important model systems [16, 43, 44]. Similarly, mouse models have also been developed using CRISPR/Cas9 approaches; in these models, tumors recapitulate some key features of human FLC, but they grow slowly, limiting their use [27, 28]. Organoids derived from tumors have only been recently described [45, 46]. Here we engineered a new mouse allele in which the DNAJ1B-PKA fusion can be induced following Cre-mediated recombination in transgenic mice. We used this new model to investigate the consequences of DNAJ1B-PKA expression in the adult liver. We were able to develop allografts and 3D culture systems that are amenable to investigations exploring further the biology of FLC and identifying new therapeutic approaches.

RESULTS

Transgenic mice expressing DNAJ1B-PKA

We generated transgenic mice by inserting a *DNAJB1-PRKACA-GFP* cDNA into the *Rosa26* locus. Upon Cre-mediated recombination and self-cleaving of the fusion protein, this construct allows expression of the DNAJB1-PKA fusion found in human FLC and the GFP reporter (**Fig. 1A**). *Rosa26*$^{LSL\text{-}DNAJB1\text{-}PKA}$ transgenic mice were healthy and fertile, as would be expected for a conditional allele.

The cell of origin of FLC cannot be determined conclusively from patients. While mouse models have shown that adult hepatocytes can initiate FLC [27, 28], the development of FLC in young patients and the expression of stem cell markers in these tumors [3, 13-17, 44] are also suggestive of an initiating event early in liver

development. We wondered if expression of the DNAJB1-PKA fusion in the developing liver may initiate FLC more frequently and more rapidly than in the adult setting. To test this idea, we crossed *Rosa26*$^{LSL\text{-}DNAJB1\text{-}PKA\text{-}GFP}$ mice to *Alb-Cre* mice where the Cre recombinase is expressed under the control of the *Albumin* promoter and is turned on at mid-gestation in the liver. Analysis of GFP expression showed positive signal in the liver of mice also expressing Cre at embryonic day E18.5 (**Fig. 1B**). Accordingly, we detected increased expression of *PRKACA* mRNA molecules in transgenic mice expressing Cre at the same time point (**Fig. 1C**).

These observations indicated proper expression of the transgene and led us to investigate the consequences of DNAJB1-PKA expression in the embryonic liver for possible tumor development later in adult mice. However, no *Alb-Cre*;*Rosa26*$^{LSL\text{-}DNAJB1\text{-}PKA\text{-}GFP}$ pups from this cross survived past weaning (**Fig. 1D**).

Expression of DNAJ1B-PKA in the embryonic liver leads to developmental defects

As a first step to understand the cause underlying this perinatal death, we performed RNA sequencing (RNA-seq) from livers dissected from control and transgenic embryos at embryonic day 18.5 (E18.5). The analysis of these data confirmed expression of the fusion transcript in the transgenic livers (**Fig. S1A,B**). We identified 331 genes significantly downregulated and 240 genes significantly upregulated in *Alb-Cre* *Rosa26*$^{LSL\text{-}DNAJB1\text{-}PKA\text{-}GFP}$ E18.5 livers compared to controls (**Table S1**). Gene ontology (GO) term analysis showed an enrichment for processes related to inflammation and metabolism, including fatty acid metabolism (**Fig. 1E** and **Table S2**). This analysis was suggestive of differences in liver development. Indeed, when we examined the expression of genes expressed at different stages and in different cell types during liver development [47], we found that a number of genes related to hepatocytes were upregulated in transgenic livers compared to controls. This included *Afp* (coding for Alpha-fetoprotein), *Arg1* (coding for Arginase-1), *Krt18* (coding for cytokeratin 18), as well as genes coding for enzymes implicated in gluconeogenesis (e.g., *Tat* for tyrosine transaminase and *Pck1* coding for phosphoenolpyruvate carboxykinase 1) (**Fig. 1F** and **Table S1**). In contrast, we noted a downregulation of genes coding for markers of

cholangiocytes, including *Sox9*, *Krt7* and *Krt19* coding for cytokeratins 7 and 19, and *Cyp7a1* coding for cholesterol 7 alpha-hydroxylase; there was also upregulation of the neuroendocrine gene *Chgb*, which codes for Chromogranin B; neuroendocrine gene programs have been associated with injured liver phenotypes [48] (**Fig. 1F** and **Table S1**).

These observations indicate that expression of the DNAJB1-PKA fusion in *Albumin*-positive liver cells results in developmental phenotypes that are incompatible with survival.

DNAJ1B-PKA expression in the adult liver of mice results in the development of slow-growing tumors with low penetrance

Fluorescence in situ hybridization (FISH) shows that the gene fusion is only present in FLC cells and not in surrounding liver cells [49]. To introduce the oncogenic fusion in a subset of adult liver cells and allow for clonal growth, we performed hydrodynamic tail vein tail injections of *Rosa26*$^{LSL\text{-}DNAJB1\text{-}PKA\text{-}GFP}$ mice with a plasmid expressing the Cre recombinase (**Fig. 2A**), generating a cohort of 38 animals (28 males and 10 females). We aged these mice and waited for signs of disease before analysis. We found that 10 mice developed tumors (3 spleen tumors, which were not further studied, and 7 liver tumors – **Table S3** and **Fig. 2B**). The low penetrance of FLC development and the slow growth of these tumors in this transgenic model is consistent with previously described mouse models [27, 28], and makes it difficult to use these mice as pre-clinical models of FLC development and response to candidate therapies.

We wondered if some of the most aggressive tumors in transgenic mice may be able to be transplanted into recipient mice in allograft models. We were able to generate single-cell suspensions from tumors in 5 out 7 of the mice with liver tumors, 2 of which grew in NSG immunodeficient mice upon subcutaneous injection. One allograft model had a fibrosarcoma histology and was not pursued further (**Fig. S2A,B**). The other tumor, FL1 (shown in **Fig. 2B**), had histopathological features of FLC and some GFP expression by immunostaining (**Fig. S2C,D**); the first allograft generated from this primary tumor stopped growing when its size was still small and did not further expand in subsequent passages, and it was not further studied.

153 Based on this low efficiency of tumor take from single cells, we also directly
154 implanted small pieces from 2/7 tumors subcutaneously into NSG mice. These two
155 models, FL2 and FL8, grew and could be propagated into new NSG hosts. Cells in
156 these tumors were positive for the liver marker HNF4α (Hepatocyte nuclear factor 4α)
157 [50] and GFP (**Fig. 2C** and **Fig. S3A**). Similar to the two other mouse models previously
158 described [27, 28], FL2 and FL8 tumors were largely negative for the expression of
159 cytokeratins 17 and 19 (CK17/19) (**Fig. S3B**).

160 We performed bulk RNA sequencing (RNA-seq) of such passaged tumors.
161 However, when we searched for the transgene mRNA, these cell lines did not express
162 it. In addition, we analyzed the frozen stocks of FL2 and FL8 by genomic DNA PCR and
163 were not able to identify deletion of the stop cassette allowing expression of the
164 transgene (data not shown). Thus, naturally-occurring liver cancer cells likely
165 outcompeted transgene-expressing cells that may have been present in the liver of
166 aged mice.

167 DISCUSSION

168 Here we present a new transgenic mouse model for human FLC based on
169 expression of the DNAJ1B-PKA fusion protein. The *Rosa26*$^{LSL\text{-}DNAJB1\text{-}PKA}$ transgenic
170 model is versatile as Cre can be delivered at different times and in different cell types
171 using other mouse alleles or viral vectors.

172 When we activated DNAJ1B-PKA during embryonic liver development, mice did not
173 survive to adulthood, suggesting that expression of the fusion protein at this stage is
174 detrimental to some aspect of liver function. Our RNA-seq data suggest that the
175 perinatal lethality may be due to developmental defects, including possibly in bile ducts
176 but future work will be needed to investigate more thoroughly the consequences of
177 DNAJ1B-PKA expression in the embryonic liver. This lethality could be possibly
178 alleviated by decreasing the number of liver cells expressing Cre and may help initiate
179 tumors more efficiently than Cre delivery in the adult liver, for example using an *Alb-*
180 *CreER* allele with tamoxifen-inducible Cre expression [51], using low doses of tamoxifen
181 during embryogenesis. The *Rosa26*$^{LSL\text{-}DNAJB1\text{-}PKA}$ transgenic model could also be used to

182 model other cancer types in which DNAJ1B-PKA is thought to be oncogenic, including
183 rare cases of pancreatic cancer [52], which may be modeled with the appropriate Cre
184 driver.

185 A limitation of our model, similar to previous mouse models [27, 28], is the slow and
186 variable development of autochthonous tumors. It is possible that the slow growth of
187 tumors and the development of few tumors is further due to expression of GFP together
188 with the fusion protein, as GFP is immunogenic [53].A growing number of organoid and
189 patient-derived xenograft models are being developed from patients with FLC to
190 investigate key features of this disease (see [29, 30, 45, 46, 54-57] for recent
191 examples). We sought to grow FLC-like cell models in culture and as allografts from our
192 transgenic mouse model. We were able to grow some cell models, but these models did
193 not express the transgene, indicating that the expanding cell populations in this context
194 likely come from the cancerous transformation of normal liver cells with aging (and not
195 from the Cre-mediated activation of the oncogenic fusion). This further illustrates the
196 difficulty of expanding mouse FLC-like cells. Future models may need to include
197 additional genetic alterations to promote more aggressive tumor growth.

198 It has often been difficult for rare diseases such as FLC to benefit from new
199 therapies because pre-clinical models often lag compared to more frequent tumor types.
200 The development of new mouse models, but also fish models [58], may help provide
201 pre-clinical data that lead to the design of new clinical trials in patients with FLC.

202 **METHODS**

203 **Mice and generation of tumors**

204 Mice were maintained according to practices prescribed by the NIH at Stanford's
205 Research Animal Facility (approved protocol #32398). Additional accreditation of
206 Stanford animal research facilities was provided by the Association for Assessment and
207 Accreditation of Laboratory Animal Care (AAALAC).

208 A *Rosa26*$^{LSL\text{-}DNAJB1\text{-}PKA\text{-}GFP}$ C56BL/6 founder mouse was generated and validated by
209 Applied StemCell using a site-specific integrase via pronuclear injection [59]. *Alb-Cre*
210 mice were described before [60] and obtained from the Jackson Laboratory (Stock No:
211 035593). Primers for genotyping are available upon request.

212 To generate tumors in the liver of mice, 10-16-week-old mice were anesthetized using
213 isoflurane, the tail vein was dilated with a heat pad, and 10 µg of Turbo-Cre plasmid
214 was delivered in a solution of sterile PBS using a hydrodynamic tail-vein injection
215 protocol. The Turbo-Cre plasmid was a gift from the laboratory of Dr. Steven Artandi at
216 Stanford University. Mice were housed for 1-2 years before subsequent analysis.

217 **RT-qPCR**

218 Liver tissue was isolated by microdissection, minced with a razor blade, and total RNA
219 was collected using RNeasy Fibrous Tissue Mini Kit (Qiagen). cDNA synthesis was
220 performed using the iScript cDNA synthesis kit (Bio-Rad) and RT-qPCR was performed
221 using iQ SYBRGreen supermix (Bio-Rad). The following RT-qPCR primers were used
222 DNAJPRKACA F: 5'-TTACTACCAGACGTTGGGCCT-3', DNAJPRKACA R: 5'-
223 ATAGTGGTTCCCGGTCTCCT-3', mPRKACA-aF: 5'-AGATCGTCCTGACCTTTGAGT-
224 3', mPRKACA-aR: 5'-GGCAAAACCGAAGTCTGTCAC-3', mPRKACA-bF: 5'-
225 GGTGACAGACTTCGGTTTTGC-3', mPRKACA-bR: 5'-
226 CACAGCCTTGTTGTAGCCTTT-3'.

227 **Immunostaining**

228 Tissues were fixed with 4% paraformaldehyde (PFA) in phosphate-buffered saline
229 (PBS). Liver tissues (normal or tumor) were initially perfused with 10 mL PFA through

230 the inferior vena cava. All tissues were submerged in 4% PFA for 48 hr before being
231 switched to 70% ethanol and finally processed and embedded. Slides were
232 deparaffinized in 2x 5 min changes of Histo-Clear (National Diagnostics HS-202), and
233 rehydrated in 2x 1 min changes of 100% ethanol, 2x 1 min changes of 70% ethanol,
234 and finally 2x 5 min changes of distilled water. Antigen retrieval was performed in a
235 microwave for 10 min with citrate-based buffer (Vector Labs H-3300). Slides were
236 cooled at room temperature, quenched for endogenous enzyme activity (SP-6000), and
237 washed in 3x 3 min changes of PBS with 0.1% Tween-20 (PBST) (Sigma P1379).
238 Slides were blocked with secondary antibody serum for 1 hr at room temperature (RT).
239 The GFP antibody (Cell Signaling Technology #2956) was diluted to 1:200 in PBST and
240 applied to slides for 1 hr at 37 ºC. Slides were washed in 3x 3 min changes of PBST.
241 Horse anti-rabbit secondary (Vector Labs MP-7401) was applied to slides for 1 hr at 37
242 ºC. Slides were washed in 3x 3 min changes of PBST. The chromogen was developed
243 using a DAB substrate kit (Vector SK-4100) for 5 min before quenching in distilled water
244 for 5 min. Slides were counterstained with hematoxylin (Newcomer Supply 1201B,
245 dehydrated in 2x 1 min changes of 70% ethanol, 2x 1 min changes of 100% ethanol,
246 and finally cleared in 2x 5 min changes of xylene before mounting.

247 Embryos were dissected from timed pregnant females, fixed in 4% PFA overnight and
248 sections were generated as described above. Sections were depaffarinized, rehydrated,
249 and tissue was blocked in 5% goat serum for 1 hr. Anti-GFP was added overnight. The
250 following day, samples were washed before incubation with Goat anti-Rabbit - Alexa
251 Fluor™ 488 (Thermo Fisher Scientific) and DAPI (Sigma). Samples were washed and
252 mounted in ProLong Gold mounting media (Thermo Fisher Scientific) before confocal
253 imaging.

254 **Tumor transplantation studies**

255 Nod.Cg-Prkdc^{scid}IL2rg^{tm1Wjl}/SzJ (NSG) mice (Jackson Laboratories, Stock No: 005557)
256 were used for all experiments in immunodeficient recipients.

257 Tumors from *Rosa26*$^{LSL\text{-}DNAJB1\text{-}PKA\text{-}GFP}$ mice were microdissected from livers or lungs.
258 Tumors were bisected once to increase surface area exposed to transplant media
259 (Kubota's medium) and kept on ice until ready for transplant. Recipient mice were

anesthetized. The shaved flank was sterilized with one swab of betadine, one swab of 70% ethanol repeated 3 times. After confirming adequate depth of anesthesia by toe-pinch, a 5 mm incision was made in the shaved flank. Blunt dissection under the skin was used to separate the skin from the muscle, creating a pocket between the 2 layers. Tumor pieces were implanted (bisected side facing the muscular wall, ~5 mm piece) near macroscopically visible capillaries on muscle wall. The incision was closed using 9 mm wound clips. For orthotopic injections, cells were disaggregated from Matrigel using the protocol described above**.** Cell pellets were resuspended at a concentration of 10^4-10^5 cells in 25 µL. These cell suspensions were mixed with an equivalent volume of Matrigel to a total volume of 50 µL. Mice were anesthetized and shaved in the abdomen. Lateral incision was made in the skin directly inferior to xyphoid process. Blunt dissection was used to separate surrounding skin from parenchyma and musculature. Incision was made in caudal direction originating from xyphoid process. The largest liver lobe available was exposed and stabilized. For cell injection, 20 µL of cells mixed 1:1 with Matrigel were injected. For tissue implantation, tissue 3-8 mm-wide at longest axis was sutured to the liver lobe using 5-0 vicryl suture. Liver lobe was returned to original site. Mouse musculature was closed with 5-0 vicryl running suture, skin was closed with 9mm wound clips.

RNA sequencing analysis

Frozen tumor samples were sent to Novogene for RNA extraction and library preparation. Raw sequencing reads were demultiplexed by the vendor to generate approximately 20 million paired-end reads per sample. Fastq files were trimmed using CutAdapt (v2.10) [61] using TruSeq sequencing adapter (5'-AGATCGGAAGAGCACACGTCTGAACTCCAGTCAC-3'), and a minimum read length of at least 25. Reads were then aligned to the ENSEMBL mm10 genome using HiSat2 [62] using reverse strandedness and discarding unaligned reads. Counts were assigned to genes using featureCounts [63] at ENSEMBL gene annotation (v93). Differential expression analysis was conducted using DESeq2 [64] on R v4.1.2 (https://www.R-project.org/).

Statistics and reproducibility

Statistical significance was assessed using the Prism GraphPad software. The specific tests used are indicated in the figure legends. Investigators were not blinded to allocation during experiments and outcome assessment.

Data availability

All RNA sequencing datasets generated in this study are available at Gene Expression Omnibus (GEO) under Super Series GSE249325 (https://www.ncbi.nlm.nih.gov/geo/query/acc.cgi?acc=GSE249325). All other data are available in the article and supplementary materials, or from the corresponding author upon reasonable request.

ACKNOWLEDGMENTS

We thank Pauline Chu from the histology facility for her help with tissue sections and all the members of the Sage lab for their help and support throughout this study. Research reported in this publication was supported by grants from the Fibrolamellar Cancer Foundation and the Alex's Lemonade Stand Foundation. J.S. is the Elaine and John Chambers Professor in Pediatric Cancer.

REFERENCES

1. Yang JD, Hainaut P, Gores GJ, Amadou A, Plymoth A, Roberts LR. A global view of hepatocellular carcinoma: trends, risk, prevention and management. Nat Rev Gastroenterol Hepatol. 2019;16(10):589-604. Epub 2019/08/24. doi: 10.1038/s41575-019-0186-y. PubMed PMID: 31439937; PubMed Central PMCID: PMCPMC6813818.

2. Ranganathan S, Lopez-Terrada D, Alaggio R. Hepatoblastoma and Pediatric Hepatocellular Carcinoma: An Update. Pediatr Dev Pathol. 2020;23(2):79-95. Epub 2019/09/27. doi: 10.1177/1093526619875228. PubMed PMID: 31554479.

3. Ward SC, Waxman S. Fibrolamellar carcinoma: a review with focus on genetics and comparison to other malignant primary liver tumors. Semin Liver Dis. 2011;31(1):61-70. Epub 2011/02/24. doi: 10.1055/s-0031-1272835. PubMed PMID: 21344351.

4. Chakrabarti S, Tella SH, Kommalapati A, Huffman BM, Yadav S, Riaz IB, et al. Clinicopathological features and outcomes of fibrolamellar hepatocellular carcinoma. J Gastrointest Oncol. 2019;10(3):554-61. Epub 2019/06/12. doi: 10.21037/jgo.2019.01.35. PubMed PMID: 31183207; PubMed Central PMCID: PMCPMC6534717.

5. O'Neill AF, Church AJ, Perez-Atayde AR, Shaikh R, Marcus KJ, Vakili K. Fibrolamellar carcinoma: An entity all its own. Curr Probl Cancer. 2021;45(4):100770. Epub 20210701. doi: 10.1016/j.currproblcancer.2021.100770. PubMed PMID: 34272087.

6. Njei B, Konjeti VR, Ditah I. Prognosis of Patients With Fibrolamellar Hepatocellular Carcinoma Versus Conventional Hepatocellular Carcinoma: A Systematic Review and Meta-analysis. Gastrointestinal cancer research : GCR. 2014;7(2):49-54. Epub 2014/05/07. PubMed PMID: 24799971; PubMed Central PMCID: PMC4007676.

7. Stevens WR, Johnson CD, Stephens DH, Nagorney DM. Fibrolamellar hepatocellular carcinoma: stage at presentation and results of aggressive surgical management. AJR Am J Roentgenol. 1995;164(5):1153-8. Epub 1995/05/01. doi: 10.2214/ajr.164.5.7717223. PubMed PMID: 7717223.

8. Katzenstein HM, Krailo MD, Malogolowkin MH, Ortega JA, Qu W, Douglass EC, et al. Fibrolamellar hepatocellular carcinoma in children and adolescents. Cancer. 2003;97(8):2006-12. Epub 2003/04/04. doi: 10.1002/cncr.11292. PubMed PMID: 12673731.

9. Ang CS, Kelley RK, Choti MA, Cosgrove DP, Chou JF, Klimstra D, et al. Clinicopathologic characteristics and survival outcomes of patients with fibrolamellar carcinoma: data from the fibrolamellar carcinoma consortium. Gastrointestinal cancer research : GCR. 2013;6(1):3-9. Epub 2013/03/19. PubMed PMID: 23505572; PubMed Central PMCID: PMC3597938.

10. Chun YS, Zimmitti G. Fibrolamellar variant of hepatocellular carcinoma. Recent results in cancer research Fortschritte der Krebsforschung Progres dans les recherches

344 sur le cancer. 2013;190:101-10. Epub 2012/09/04. doi: 10.1007/978-3-642-16037-0_7.
345 PubMed PMID: 22941016.

346 11. Craig JR, Peters RL, Edmondson HA, Omata M. Fibrolamellar carcinoma of the
347 liver: a tumor of adolescents and young adults with distinctive clinico-pathologic
348 features. Cancer. 1980;46(2):372-9. Epub 1980/07/15. PubMed PMID: 6248194.

349 12. Liu S, Chan KW, Wang B, Qiao L. Fibrolamellar hepatocellular carcinoma. Am J
350 Gastroenterol. 2009;104(10):2617-24; quiz 25. Epub 2009/07/30. doi:
351 10.1038/ajg.2009.440. PubMed PMID: 19638962.

352 13. Yamashita T, Forgues M, Wang W, Kim JW, Ye Q, Jia H, et al. EpCAM and
353 alpha-fetoprotein expression defines novel prognostic subtypes of hepatocellular
354 carcinoma. Cancer Res. 2008;68(5):1451-61. Epub 2008/03/05. doi: 68/5/1451 [pii]
355 10.1158/0008-5472.CAN-07-6013. PubMed PMID: 18316609.

356 14. Ward SC, Huang J, Tickoo SK, Thung SN, Ladanyi M, Klimstra DS. Fibrolamellar
357 carcinoma of the liver exhibits immunohistochemical evidence of both hepatocyte and
358 bile duct differentiation. Mod Pathol. 2010;23(9):1180-90. Epub 2010/05/25. doi:
359 10.1038/modpathol.2010.105. PubMed PMID: 20495535.

360 15. Ross HM, Daniel HD, Vivekanandan P, Kannangai R, Yeh MM, Wu TT, et al.
361 Fibrolamellar carcinomas are positive for CD68. Mod Pathol. 2011;24(3):390-5. Epub
362 2010/11/30. doi: 10.1038/modpathol.2010.207. PubMed PMID: 21113139; PubMed
363 Central PMCID: PMC3292186.

364 16. Oikawa T, Kamiya A, Zeniya M, Chikada H, Hyuck AD, Yamazaki Y, et al. Sal-
365 like protein 4 (SALL4), a stem cell biomarker in liver cancers. Hepatology.
366 2013;57(4):1469-83. Epub 2012/11/24. doi: 10.1002/hep.26159. PubMed PMID:
367 23175232.

368 17. Van Eyken P, Sciot R, Brock P, Casteels-Van Daele M, Ramaekers FC, Desmet
369 VJ. Abundant expression of cytokeratin 7 in fibrolamellar carcinoma of the liver.
370 Histopathology. 1990;17(2):101-7. Epub 1990/08/01. PubMed PMID: 1699871.

371 18. Berman MA, Burnham JA, Sheahan DG. Fibrolamellar carcinoma of the liver: an
372 immunohistochemical study of nineteen cases and a review of the literature. Hum
373 Pathol. 1988;19(7):784-94. doi: 10.1016/s0046-8177(88)80261-2. PubMed PMID:
374 2456977.

375 19. Alshareefy Y, Shen CY, Prekash RJ. Exploring the molecular pathogenesis,
376 diagnosis and treatment of fibrolamellar hepatocellular carcinoma: A state of art review
377 of the current literature. Pathol Res Pract. 2023;248:154655. Epub 20230626. doi:
378 10.1016/j.prp.2023.154655. PubMed PMID: 37429175.

379 20. Honeyman JN, Simon EP, Robine N, Chiaroni-Clarke R, Darcy DG, Lim, II, et al.
380 Detection of a recurrent DNAJB1-PRKACA chimeric transcript in fibrolamellar
381 hepatocellular carcinoma. Science. 2014;343(6174):1010-4. Epub 2014/03/01. doi:
382 10.1126/science.1249484. PubMed PMID: 24578576.

383 21. Simon SM. Fighting rare cancers: lessons from fibrolamellar hepatocellular
384 carcinoma. Nature Reviews Cancer. 2023;23(5):335-46. Epub 2023 Mar 17. doi:
385 10.1038/s41568-023-00554-w.

386 22. Cornella H, Alsinet C, Sayols S, Zhang Z, Hao K, Cabellos L, et al. Unique
387 genomic profile of fibrolamellar hepatocellular carcinoma. Gastroenterology.
388 2015;148(4):806-18 e10. Epub 2015/01/06. doi: 10.1053/j.gastro.2014.12.028. PubMed
389 PMID: 25557953; PubMed Central PMCID: PMCPMC4521774.

390 23. Xu L, Hazard FK, Zmoos AF, Jahchan N, Chaib H, Garfin PM, et al. Genomic
391 analysis of fibrolamellar hepatocellular carcinoma. Hum Mol Genet. 2015;24(1):50-63.
392 doi: 10.1093/hmg/ddu418. PubMed PMID: 25122662; PubMed Central PMCID:
393 PMCPMC4262492.

394 24. Graham RP, Jin L, Knutson DL, Kloft-Nelson SM, Greipp PT, Waldburger N, et
395 al. DNAJB1-PRKACA is specific for fibrolamellar carcinoma. Mod Pathol.
396 2015;28(6):822-9. doi: 10.1038/modpathol.2015.4. PubMed PMID: 25698061.

397 25. Graham RP, Lackner C, Terracciano L, Gonzalez-Cantu Y, Maleszewski JJ,
398 Greipp PT, et al. Fibrolamellar carcinoma in the Carney complex: PRKAR1A loss
399 instead of the classic DNAJB1-PRKACA fusion. Hepatology. 2018;68(4):1441-7. Epub
400 2017/12/10. doi: 10.1002/hep.29719. PubMed PMID: 29222914; PubMed Central
401 PMCID: PMCPMC6151295.

402 26. Hirsch TZ, Negulescu A, Gupta B, Caruso S, Noblet B, Couchy G, et al. BAP1
403 mutations define a homogeneous subgroup of hepatocellular carcinoma with
404 fibrolamellar-like features and activated PKA. J Hepatol. 2020;72(5):924-36. Epub
405 2019/12/22. doi: 10.1016/j.jhep.2019.12.006. PubMed PMID: 31862487.

406 27. Kastenhuber ER, Lalazar G, Houlihan SL, Tschaharganeh DF, Baslan T, Chen
407 CC, et al. DNAJB1-PRKACA fusion kinase interacts with beta-catenin and the liver
408 regenerative response to drive fibrolamellar hepatocellular carcinoma. Proc Natl Acad
409 Sci U S A. 2017;114(50):13076-84. doi: 10.1073/pnas.1716483114. PubMed PMID:
410 29162699.

411 28. Engelholm LH, Riaz A, Serra D, Dagnaes-Hansen F, Johansen JV, Santoni-
412 Rugiu E, et al. CRISPR/Cas9 Engineering of Adult Mouse Liver Demonstrates That the
413 Dnajb1-Prkaca Gene Fusion Is Sufficient to Induce Tumors Resembling Fibrolamellar
414 Hepatocellular Carcinoma. Gastroenterology. 2017;153(6):1662-73 e10. doi:
415 10.1053/j.gastro.2017.09.008. PubMed PMID: 28923495.

416 29. Toyota A, Goto M, Miyamoto M, Nagashima Y, Iwasaki S, Komatsu T, et al.
417 Novel protein kinase cAMP-Activated Catalytic Subunit Alpha (PRKACA) inhibitor
418 shows anti-tumor activity in a fibrolamellar hepatocellular carcinoma model. Biochem
419 Biophys Res Commun. 2022;621:157-61. Epub 2022/07/16. doi:
420 10.1016/j.bbrc.2022.07.008. PubMed PMID: 35839742.

421 30. Neumayer C, Ng D, Jiang CS, Qureshi A, Lalazar G, Vaughan R, et al.
422 Oncogenic Addiction of Fibrolamellar Hepatocellular Carcinoma to the Fusion Kinase
423 DNAJB1-PRKACA. Clin Cancer Res. 2023;29(1):271-8. doi: 10.1158/1078-0432.CCR-
424 22-1851. PubMed PMID: 36302174; PubMed Central PMCID: PMCPMC9811160.

425 31. Cao B, Lu TW, Martinez Fiesco JA, Tomasini M, Fan L, Simon SM, et al.
426 Structures of the PKA RIalpha Holoenzyme with the FLHCC Driver J-PKAcalpha or
427 Wild-Type PKAcalpha. Structure. 2019;27(5):816-28 e4. Epub 2019/03/25. doi:

428 10.1016/j.str.2019.03.001. PubMed PMID: 30905674; PubMed Central PMCID:
429 PMCPMC6506387.

430 32. Lu TW, Aoto PC, Weng JH, Nielsen C, Cash JN, Hall J, et al. Structural analyses
431 of the PKA RIIbeta holoenzyme containing the oncogenic DnaJB1-PKAc fusion protein
432 reveal protomer asymmetry and fusion-induced allosteric perturbations in fibrolamellar
433 hepatocellular carcinoma. PLoS Biol. 2020;18(12):e3001018. Epub 2020/12/29. doi:
434 10.1371/journal.pbio.3001018. PubMed PMID: 33370777; PubMed Central PMCID:
435 PMCPMC7793292.

436 33. Olivieri C, Walker C, Karamafrooz A, Wang Y, Manu VS, Porcelli F, et al.
437 Defective internal allosteric network imparts dysfunctional ATP/substrate-binding
438 cooperativity in oncogenic chimera of protein kinase A. Commun Biol. 2021;4(1):321.
439 Epub 2021/03/12. doi: 10.1038/s42003-021-01819-6. PubMed PMID: 33692454;
440 PubMed Central PMCID: PMCPMC7946884.

441 34. Zhang JZ, Lu TW, Stolerman LM, Tenner B, Yang JR, Zhang JF, et al. Phase
442 Separation of a PKA Regulatory Subunit Controls cAMP Compartmentation and
443 Oncogenic Signaling. Cell. 2020;182(6):1531-44 e15. Epub 2020/08/28. doi:
444 10.1016/j.cell.2020.07.043. PubMed PMID: 32846158; PubMed Central PMCID:
445 PMCPMC7502557.

446 35. Turnham RE, Smith FD, Kenerson HL, Omar MH, Golkowski M, Garcia I, et al.
447 An acquired scaffolding function of the DNAJ-PKAc fusion contributes to oncogenic
448 signaling in fibrolamellar carcinoma. Elife. 2019;8. Epub 2019/05/08. doi:
449 10.7554/eLife.44187. PubMed PMID: 31063128; PubMed Central PMCID:
450 PMCPMC6533061.

451 36. Piette BL, Alerasool N, Lin ZY, Lacoste J, Lam MHY, Qian WW, et al.
452 Comprehensive interactome profiling of the human Hsp70 network highlights functional
453 differentiation of J domains. Mol Cell. 2021;81(12):2549-65 e8. Epub 2021/05/07. doi:
454 10.1016/j.molcel.2021.04.012. PubMed PMID: 33957083.

455 37. Trankenschuh W, Puls F, Christgen M, Albat C, Heim A, Poczkaj J, et al.
456 Frequent and distinct aberrations of DNA methylation patterns in fibrolamellar
457 carcinoma of the liver. PLoS One. 2010;5(10):e13688. Epub 2010/11/10. doi:
458 10.1371/journal.pone.0013688. PubMed PMID: 21060828; PubMed Central PMCID:
459 PMC2966398.

460 38. Dinh TA, Sritharan R, Smith FD, Francisco AB, Ma RK, Bunaciu RP, et al.
461 Hotspots of Aberrant Enhancer Activity in Fibrolamellar Carcinoma Reveal Candidate
462 Oncogenic Pathways and Therapeutic Vulnerabilities. Cell Rep. 2020;31(2):107509.
463 Epub 2020/04/16. doi: 10.1016/j.celrep.2020.03.073. PubMed PMID: 32294439;
464 PubMed Central PMCID: PMCPMC7474926.

465 39. El Dika I, Bowman AS, Berger MF, Capanu M, Chou JF, Benayed R, et al.
466 Molecular profiling and analysis of genetic aberrations aimed at identifying potential
467 therapeutic targets in fibrolamellar carcinoma of the liver. Cancer. 2020;126(18):4126-
468 35. Epub 2020/07/15. doi: 10.1002/cncr.32960. PubMed PMID: 32663328.

469 40. Kannangai R, Vivekanandan P, Martinez-Murillo F, Choti M, Torbenson M.
470 Fibrolamellar carcinomas show overexpression of genes in the RAS, MAPK, PIK3, and

xenobiotic degradation pathways. Hum Pathol. 2007;38(4):639-44. Epub 2007/03/21. doi: 10.1016/j.humpath.2006.07.019. PubMed PMID: 17367606.

41. Hirsch TZ, Pilet J, Morcrette G, Roehrig A, Monteiro BJ, Molina L, et al. Integrated genomic analysis identifies driver genes and cisplatin-resistant progenitor phenotype in pediatric liver cancer. Cancer Discov. 2021. Epub 2021/04/25. doi: 10.1158/2159-8290.CD-20-1809. PubMed PMID: 33893148.

42. Dinh TA, Utria AF, Barry KC, Ma R, Abou-Alfa GK, Gordan JD, et al. A framework for fibrolamellar carcinoma research and clinical trials. Nat Rev Gastroenterol Hepatol. 2022;19(5):328-42. Epub 2022/02/23. doi: 10.1038/s41575-022-00580-3. PubMed PMID: 35190728.

43. Dinh TA, Jewell ML, Kanke M, Francisco A, Sritharan R, Turnham RE, et al. MicroRNA-375 Suppresses the Growth and Invasion of Fibrolamellar Carcinoma. Cell Mol Gastroenterol Hepatol. 2019;7(4):803-17. Epub 2019/02/15. doi: 10.1016/j.jcmgh.2019.01.008. PubMed PMID: 30763770; PubMed Central PMCID: PMCPMC6468197.

44. Oikawa T, Wauthier E, Dinh TA, Selitsky SR, Reyna-Neyra A, Carpino G, et al. Model of fibrolamellar hepatocellular carcinomas reveals striking enrichment in cancer stem cells. Nat Commun. 2015;6:8070. doi: 10.1038/ncomms9070. PubMed PMID: 26437858.

45. Narayan NJC, Requena D, Lalazar G, Ramos-Espiritu L, Ng D, Levin S, et al. Human liver organoids for disease modeling of fibrolamellar carcinoma. Stem Cell Reports. 2022. Epub 2022/07/09. doi: 10.1016/j.stemcr.2022.06.003. PubMed PMID: 35803261.

46. Ruland L, Andreatta F, Massalini S, Chuva de Sousa Lopes S, Clevers H, Hendriks D, et al. Organoid models of fibrolamellar carcinoma mutations reveal hepatocyte transdifferentiation through cooperative BAP1 and PRKAR2A loss. Nat Commun. 2023;14(1):2377. Epub 20230503. doi: 10.1038/s41467-023-37951-6. PubMed PMID: 37137901; PubMed Central PMCID: PMCPMC10156813.

47. Chaudhari P, Tian L, Deshmukh A, Jang YY. Expression kinetics of hepatic progenitor markers in cellular models of human liver development recapitulating hepatocyte and biliary cell fate commitment. Exp Biol Med (Maywood). 2016;241(15):1653-62. Epub 20160706. doi: 10.1177/1535370216657901. PubMed PMID: 27390263; PubMed Central PMCID: PMCPMC4999623.

48. Alvaro D, Mancino MG, Glaser S, Gaudio E, Marzioni M, Francis H, et al. Proliferating cholangiocytes: a neuroendocrine compartment in the diseased liver. Gastroenterology. 2007;132(1):415-31. Epub 20060724. doi: 10.1053/j.gastro.2006.07.023. PubMed PMID: 17241889.

49. Weiel JJ, Forgo B, Sage J, Rangaswami A, Hazard FK. The Use of Fluorescence in situ Hybridization to Confirm PRKACA Gene Rearrangement in Fibrolamellar Hepatocellular Carcinoma: A Validation Study. Ann Clin Lab Sci. 2022;52(3):475-83. PubMed PMID: 35777788.

50. Walesky C, Apte U. Role of hepatocyte nuclear factor 4alpha (HNF4alpha) in cell proliferation and cancer. Gene Expr. 2015;16(3):101-8. Epub 2015/02/24. doi: 10.3727/105221615X14181438356292. PubMed PMID: 25700366; PubMed Central PMCID: PMCPMC5841246.

51. Schuler M, Dierich A, Chambon P, Metzger D. Efficient temporally controlled targeted somatic mutagenesis in hepatocytes of the mouse. Genesis. 2004;39(3):167-72. Epub 2004/07/30. doi: 10.1002/gene.20039. PubMed PMID: 15282742.

52. Vyas M, Hechtman JF, Zhang Y, Benayed R, Yavas A, Askan G, et al. DNAJB1-PRKACA fusions occur in oncocytic pancreatic and biliary neoplasms and are not specific for fibrolamellar hepatocellular carcinoma. Mod Pathol. 2020;33(4):648-56. Epub 20191101. doi: 10.1038/s41379-019-0398-2. PubMed PMID: 31676785; PubMed Central PMCID: PMCPMC7125037.

53. Grzelak CA, Goddard ET, Lederer EE, Rajaram K, Dai J, Shor RE, et al. Elimination of fluorescent protein immunogenicity permits modeling of metastasis in immune-competent settings. Cancer Cell. 2022;40(1):1-2. Epub 20211202. doi: 10.1016/j.ccell.2021.11.004. PubMed PMID: 34861158; PubMed Central PMCID: PMCPMC9668376.

54. Zhang W, Xu Y, Wang X, Oikawa T, Su G, Wauthier E, et al. Fibrolamellar carcinomas-growth arrested by paracrine signals complexed with synthesized 3-O sulfated heparan sulfate oligosaccharides. Matrix Biol. 2023;121:194-216. Epub 20230702. doi: 10.1016/j.matbio.2023.06.008. PubMed PMID: 37402431.

55. Shebl B, Ng D, Lalazar G, Rosemore C, Finkelstein TM, Migler RD, et al. Targeting BCL-XL in fibrolamellar hepatocellular carcinoma. JCI Insight. 2022;7(17). Epub 20220908. doi: 10.1172/jci.insight.161820. PubMed PMID: 36073545; PubMed Central PMCID: PMCPMC9536265.

56. Leiting JL, Hernandez MC, Bergquist JR, Yonkus JA, Abdelrahman AM, Torbenson MS, et al. Therapeutic Efficacy of Temsirolimus in a Patient-derived Model of Metastatic Fibrolamellar Hepatocellular Carcinoma. In Vivo. 2023;37(5):1940-50. doi: 10.21873/invivo.13290. PubMed PMID: 37652480; PubMed Central PMCID: PMCPMC10500502.

57. Lalazar G, Requena D, Ramos-Espiritu L, Ng D, Bhola PD, de Jong YP, et al. Identification of Novel Therapeutic Targets for Fibrolamellar Carcinoma Using Patient-Derived Xenografts and Direct-from-Patient Screening. Cancer Discov. 2021;11(10):2544-63. Epub 20210614. doi: 10.1158/2159-8290.CD-20-0872. PubMed PMID: 34127480; PubMed Central PMCID: PMCPMC8734228.

58. de Oliveira S, Houseright RA, Korte BG, Huttenlocher A. DnaJ-PKAc fusion induces liver inflammation in a zebrafish model of fibrolamellar carcinoma. Dis Model Mech. 2020;13(4). Epub 20200430. doi: 10.1242/dmm.042564. PubMed PMID: 32102783; PubMed Central PMCID: PMCPMC7197716.

59. Tasic B, Hippenmeyer S, Wang C, Gamboa M, Zong H, Chen-Tsai Y, et al. Site-specific integrase-mediated transgenesis in mice via pronuclear injection. Proc Natl Acad Sci U S A. 2011;108(19):7902-7. doi: 10.1073/pnas.1019507108. PubMed PMID: 21464299; PubMed Central PMCID: PMCPMC3093482.

555 60. Postic C, Shiota M, Niswender KD, Jetton TL, Chen Y, Moates JM, et al. Dual
556 roles for glucokinase in glucose homeostasis as determined by liver and pancreatic beta
557 cell-specific gene knock-outs using Cre recombinase. J Biol Chem. 1999;274(1):305-15.
558 Epub 1998/12/29. doi: 10.1074/jbc.274.1.305. PubMed PMID: 9867845.

559 61. Martin M. Cutadapt removes adapter sequences from high-throughput
560 sequencing reads. EMBnet journal. 2011;17(1):10-2.

561 62. Kim D, Paggi JM, Park C, Bennett C, Salzberg SL. Graph-based genome
562 alignment and genotyping with HISAT2 and HISAT-genotype. Nat Biotechnol.
563 2019;37(8):907-15. Epub 20190802. doi: 10.1038/s41587-019-0201-4. PubMed PMID:
564 31375807; PubMed Central PMCID: PMCPMC7605509.

565 63. Liao Y, Smyth GK, Shi W. featureCounts: an efficient general purpose program
566 for assigning sequence reads to genomic features. Bioinformatics. 2014;30(7):923-30.
567 Epub 20131113. doi: 10.1093/bioinformatics/btt656. PubMed PMID: 24227677.

568 64. Love MI, Huber W, Anders S. Moderated estimation of fold change and
569 dispersion for RNA-seq data with DESeq2. Genome Biol. 2014;15(12):550. Epub
570 2014/12/18. doi: 10.1186/s13059-014-0550-8. PubMed PMID: 25516281; PubMed
571 Central PMCID: PMCPMC4302049.

FIGURE 1

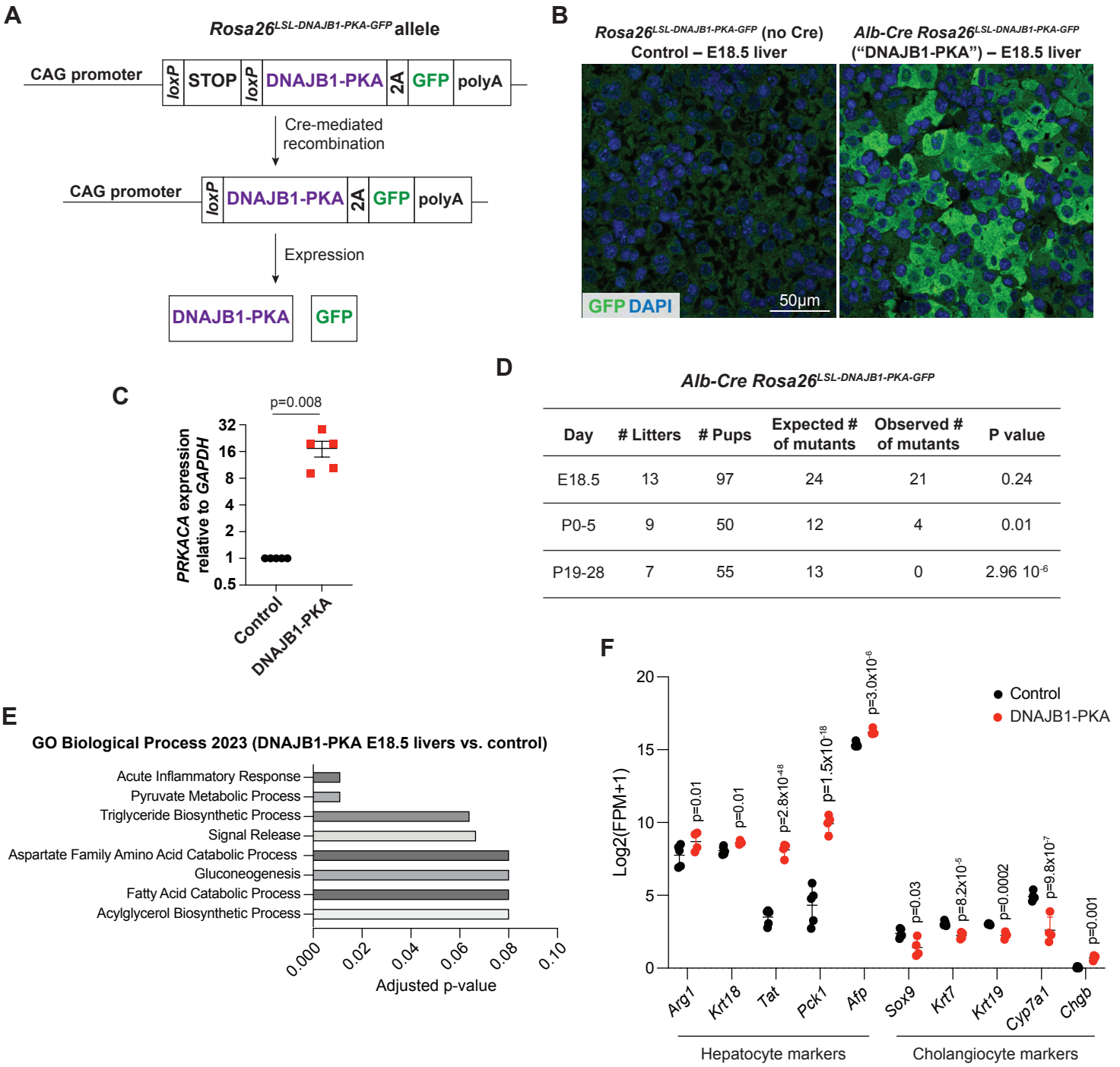

Day	# Litters	# Pups	Expected # of mutants	Observed # of mutants	P value
E18.5	13	97	24	21	0.24
P0-5	9	50	12	4	0.01
P19-28	7	55	13	0	$2.96\ 10^{-6}$

Figure 1. Generation of a transgenic mouse model to express the DNAJ1B-PRAKA fusion

A. Schematic representation of the transgene inserted into the *Rosa26* locus. The fusion cDNA is under the control of the CMV early enhancer/chicken β actin (CAG) promoter but is only expressed after Cre-mediated recombination of a transcriptional STOP cassette flanked by *loxP* sites. Upon translation, a self-cleaving 2A peptide separates the DNAJB1-PKA fusion protein from the GFP reporter. **B.** Representative confocal immunofluorescence images for GFP expression (green) from sections of control mice (transgenic mice with no Cre expression) or mice expression the fusion protein and GFP at E18.5. DAPI shows DNA staining (blue). Scale bar: 50µm. **C.** Expression levels of *PRKCA* transcripts analyzed by RT-qPCR analysis relative to *GAPDH* and to controls (n=5 E18.5 embryonic liver samples per genotype). Data shown as mean and S.E.M.; P value calculated by Mann-Whitney t-test. **D.** Analysis of expected and observed numbers of mutant mice before and after birth. P value calculated by a X^2 test. **E.** Gene Ontology (GO) analysis for biological process comparing embryonic livers at E18.5 in embryos expressing the fusion protein compared to controls. **F**. Analysis of genes related to hepatocytes and cholangiocytes in control and transgenic E18.5 livers. Data shown as mean and range. P-adjusted values are shown.

FIGURE 2

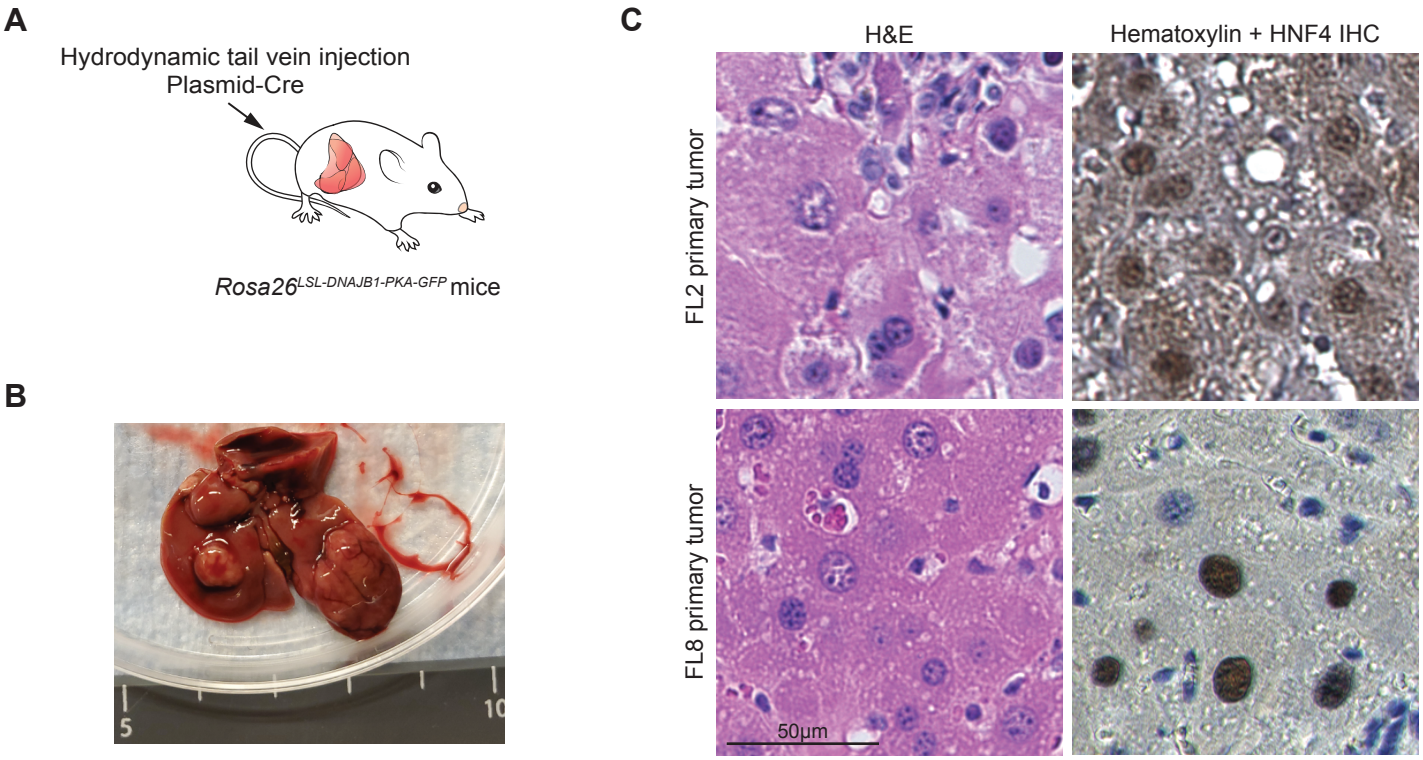

Figure 2. Propagation of tumors from transgenic mice expressing the DNAJ1B-PRAKA fusion

A. Schematic representation of the protocol to induce liver tumors in adult *Rosa26*$^{LSL\text{-}DNAJB1\text{-}PKA\text{-}GFP}$ mice upon delivery of a plasmid expressing the Cre recombinase to the liver. **B.** Representative photograph of liver tumors in the dissected liver of a *Rosa26*$^{LSL\text{-}DNAJB1\text{-}PKA\text{-}GFP}$ mouse 24.5 months after delivery of the Cre recombinase (FL1 tumor shown). **C.** Hematoxylin and eosin and hematoxylin (H&E) staining (left) and anti-HNF4α immunohistochemistry (right) on sections from the FL2 and FL8 primary tumors. Scale bar: 50µm.